Journal of Biomedical Research & Studies
Volume 4 | Issue 1

Research Article Open Access

Linear Support Vector Machine Myoelectric Pattern Recognition Control System Architecture for Transtibial Osteomyoplastic Amputees

Talon Garikayi[1*], Tawanda Mushiri[2]

[1]Biomedical Engineering Research Group, Harare Institute of Technology
[2]Department of Biomedical Engineering, University of Zimbabwe, Harare, Zimbabwe
Corresponding Author: Talon Garikayi, Biomedical Engineering Research Group, Harare Institute of Technology, E-mail: talongarikayi@gmail.com

Citation: Talon Garikayi, Tawanda Mushiri (2024) Linear Support Vector Machine Myoelectric Pattern Recognition Control System Architecture for Transtibial Osteomyoplastic Amputees, J Biomed Res Stud 4(1): 101

Received Date: November 29, 2023 **Accepted Date:** December 29, 2023 **Published Date:** January 05, 2024

Abstract

Background: The use of surface electromyography (sEMG) signals for clinical diagnosis is well appreciated in the medical field. However, the use of sEMG signals for the control of powered prosthetic limbs is still regarded as a futuristic idea. Past and present studies have focused more on the upper limb (hand) as compared to the lower limb (leg). The challenges associated with the controlling leg movement include designing for both balance and locomotion. After amputation, the muscle orientation and alignments on the residual stump changes as some of the anatomical landmarks are changed during surgical procedure. To achieve locomotion, some amputees, generally from third-world nations, use passive mechanical prosthetic limbs with a fixed ankle. These passive mechanical limbs are deemed ineffective in providing normal gait on amputees. This paper presents a novel integration of sEMG and inertial measurements to control an active powered prosthetic ankle. A pattern recognition system is presented as a technique for optimising controller performance. Furthermore, force measurements of the hind and mid foot are used to enhance the knowledge base.

Methods: Initially, passive mechanical limbs were fitted on two subjects. Reflective markers, inertial measurement units (IMU) and EMG electrodes were placed on selected anatomical landmarks and muscles respectively, for both amputated and sound leg. Vicon Nexus and Noraxon systems were used to record the data. ISEK and SENIAM standards were adhered to during data collection and processing. The results were then used to design and prototype a biomechatronic prosthetic ankle. Three sEMG signal channels and two MPU6050 IMU sensors (thigh and shank locations) were synchronised using an ADS1298 and 32-bit ARM processor. Force sensitive resistors (FSR) were placed on mid-foot and the hind-foot to aid event activation. Twenty-three time and frequency domain features were extracted and then Principal Component Analysis (PCA) was then used for dimensionality reduction. Classification gait movements was achieved through the implementation of Linear Support Vector Machine (LSVM). The biomechatronic prosthetic ankle was fitted onto the amputated leg. The subject was then tasked to perform normal gait as previously done with a passive limb. The gait parameters and anatomical angles were recorded using the Vicon Nexus and Noraxon systems simultaneously. The EMG results were further processed and analysed using the myoRESEARCH® MR3, Noraxon System.

Results: Recording of EMG signals was a challenge. Skin movement and changes in skin impedances contributed immensely to signal acquisition challenges. A high pass filter with a cut-off of 15.48Hz and low pass filter of 500 Hz was achieved. A stability analysis (Nyquist Analysis) of the circuitry produced a 0.1 factor which indicated a very stable system as evidence of acceptable common mode rejection ratio (CMRR) values of the signal amplification and processing circuitry. The wavelet denoising technique provided better signal output as compared to the Savitzky Golay and Moving Average techniques. Tibialis Anterior EMG signals were easily classified during dorsiflexion while Medialis and Gastrocnemius EMG signals were classified better during plantarflexion. During classification, 20% of the data was used for validation while 80% of the data was used for training the classifier. Principle Component analysis (PCA) was implemented as a dimensionality reduction technique in order to reduce processing time of the architecture. As a way of determining the best classifier, twenty-two classifiers were tested. Linear Support Vector Machine achieved 100% classification on labelled data and 99.25% accuracy on unknown data with a processing time of 350 ms. Ensemble classifiers exhibited a remarkable 100% classification accuracy on both trained and new data. However, their processing times were 1032.70 ms on average which is 300% more time consuming than the LSVM. Therefore, the LSVM were selected as the optimum classifier for the design. Precision, sensitivity and specificity of the LSVM were all greater than 98.9%.

Conclusion: High classification accuracy, precision, sensitivity and specificity of the LSVM provided a possibility of utilising pattern recognition control architectures for powered limbs. Input signal infidelity had a negative effect on the classifier performance. Stochastic and sinusoidal form of the sEMG signal improved the implementation of several classifier algorithms and the extraction of various types of features such as zero crossing and slope sign change. Hardware performance had an adverse effect on system performance. Therefore, if implemented in a reliable hardware system, the proposed control architecture has the capability of restoring amputee gait.

Keywords: Biomechatronics, Amputee, Osteomyoplastic, Prosthetic, Pattern recognition

Background

Lack of a healthy diet and the rising prevalence of health issues such as diabetes, as well as degenerative joint diseases such as arthritis and osteoporosis, are building the demand for prosthetics [1]. Once a patient develops degenerative joint diseases, the affected limb if not treated will ultimately result in amputation. These procedures will require use of prosthetics for rehabilitation and permanent use. In addition, traumatic events such as accidents or vascular and circulatory disorders often lead to amputation of the lower limb below the knee joint [2]. According to [3], the production cost of a transtibial mechanical passive limb for daily living activities is approximately $25 196. With basic electronic components, the cost increases to approximately $31 196. Therefore, the microprocessor-based limbs will cost close to $45 563. In South Africa, the average purchase price of a passive mechanical limb is approximately R75 000 while the cost of a powered active prosthetic is R1.4 million. As a result, the cost of prosthetic limbs is far beyond the reach of many South Africans. Therefore, the large population of South African amputees have resorted to using unorthodox methods to achieve mobility, ranging from simple walking sticks to home-made crutches.

The use of stiff mechanical prosthetic ankles causes asymmetries in gait cycle leading to possible lower back pain injuries and bruises on the load bearing points on the socket [4]. Amputees often achieve desired distance variables. However, such gait performances are achieved through the use of excessive energy and excess flexion of residual muscles to compensate for the missing limb. Thus, increased muscle contraction on the intact side and higher metabolic energy expenditure. The long-term effects are osteoarthritis, osteoporosis, back pain and to a large extent musculoskeletal problems. As a result, artificial prosthetic limbs are regarded by the amputees as exotic lifeless attachments to the body and not as a non-biological extension of the human body.

There are basically four normal requirements for gait which are equilibrium, locomotion, musculoskeletal integrity and neurological control [5]. However, as a result of amputation, amputees often struggle to achieve all the basic requirements. Mechatronic systems coupled with intelligent control architectures provide the platform to restoring an amputee's overall mobility related lifestyle. However, the recovered gait is largely influenced by the extent of amputation and functional level of the prosthesis. The transtibial osteomyoplastic amputation technique offers residual muscles that are active throughout the gait cycle. These muscles offer potential sites for extracting surface electromyography (sEMG) signals even though amputees often struggle to achieve all the basic requirements. Transtibial osteomyoplastic amputees often recover their mobility capabilities earlier than transfemoral amputees mainly due to the presence of the knee [6]. During rehabilitation different surgical procedures are usually applied depending on the cause leading to the amputation [7].

An amputee can receive a short, average (medium) or long amputation with respect to the position of amputation along the lower limb. When selecting the level of amputation there is a trade-off between increased function of the more distal level versus decreased complication rate with more proximal level [8]. As a result, as the level of amputation moves proximally, the walking speed of the individual decreases and ultimately the oxygen consumption increases. Therefore, the level of amputation has a direct impact on the recovered gait for lower limb amputees.

The motivation for osteomyoplastic amputation is the need to develop a residual limb for an amputee who is highly involved in ambulatory related activities. Therefore, there is bone bridging between the tibia and the fibula resulting in a more stable end bearing limb [9]. The loss of ankle mortise causes the fibular instability. However, the myoplasty technique brings about stability on the residual limb [10]. Furthermore, the blood flow and recovery of normal length-tension of the muscles is improved [9].

Materials and Methods

The study methods and procedures used in the study are an extract of procedures reported earlier by the same researchers in the following articles: *“Investigating the effects of passive mechanical ankle on unilateral osteomyoplastic transtibial amputees, [11]”* and *“Analysis of surface electromyography signal features on osteomyoplastic transtibial amputees for pattern recognition control architectures, [4]”*. The procedure for data collection and segmentation was explained in depth during discussion of results in this study. Furthermore, emphasis was on signal acquisition and processing since it had an influence on system performance. To achieve the desired results, the International Society of Electrophysiology and Kinesiology, ISEK [12] and Surface EMG for non-invasive assessment of muscles, SENIAM standards [13] for data collection, processing and reporting were adhered to.

Subjects

The targeted control system architecture was patient specific. Therefore, the sample size was reduced to two amputees. The sample size was reduced to two participants because the proposed solution is user specific, the mandate was simply to develop the generic framework that will require customisation upon application per patient. Since these were unilateral amputees, the right non-amputated leg was used as control. However, for the purposes of a robust pattern recognition system, the number of activities were increased and so were the samples per subject. The study was conducted under research protocol S16/05/093 approved by Health Research Ethics Committee at Stellenbosch University. The study consisted of two male unilateral transtibial amputees (left leg amputated) weighing an average of 80 ± 2 Kg and a mean height of 1.75 ± 0.02 m. The subjects were middle aged men such that subject 1 was aged 42 years and subject 2 was aged 44 years. Both the subjects had received osteomyoplastic transtibial amputation surgery. The stump length for subject 1 was 15 cm and that of subject 2 was 17 cm and the residual stumps were 33.7 % and 36 % of the sound limb respectively. The subjects had reported no history of diagnosed musculoskeletal and neurological pathology. The subjects reported independent ambulation with medium to high daily activities. The amputees had been using a passive limb for the past two years. The criteria for inclusion was based on the amputees using the assistive device in a laboratory testing environment and in the community effectively. This eliminated the need to train the subjects on how to use the limb prior to the experiments. Also considered was the need for participants with a comfortable surface bearing socket which utilises the vacuum system and had no medical history related to the limb injuries or comorbidities that could affect gait, joint angles or electromyography signals.

Apparatus and Data Acquisition

The experiments were carried out at the Human Motion Analysis Unit, Central Analytical Facilities, Stellenbosch University, South Africa. Vicon Nexus Motion Systems was used to capture the three dimensional data. A wooden floor was used to provide a smooth and soft walking platform hence improving the safety of the participant in the unfortunate event of a fall. Three force plates were correctly positioned at the middle of the walk way. The 3D positional data was also simultaneously recorded at 200 Hz using the Noraxon Myomotion System, USA. The synchronisation of the Myomotion system and Vicon Motion system data enabled data labelling as the Myomotion had a video recording system. The system was coupled to external triggers for initialising the system and automatically record the gait.

Procedure

The experimental protocol was explained both orally and in writing to all participants before written consent was obtained. The proposed system was expected to predict the intended limb movement. Hence, every limb movement was systematically associated with an expected activity to be performed. To develop a data set for the design parameters, the participants performed the following mobility related activities in the laboratory:

- Standing with both legs spread and feet pointing forward during calibration procedure.
- Walking with sEMG sensors, IMU sensors and reflective markers (Gait analysis and EMG Analysis were carried out simultaneously). The Vicon Nexus system and the Noraxon Motion system were simultaneously used in order to provide validation data.
- Sitting with sEMG sensors and performing dorsiflexion and plantarflexion movements using amputated leg.

Much attention was given to the foot, ankle, pelvis and thigh anatomical landmarks so as to clearly identify the ankle, knee and hip angles during gait. The data sets were stored as c3d files for further processing. The subjects were given enough time to walk around the laboratory and testing envelope so as to acclimatise with the environment. The subjects were tasked to perform 10 walking activities along a 10 m walking platform which had force plates mounted on the floor. The subjects were tasked to perform normal gait without any prescribed walking speed.

A pilot study was carried out to determine the best possible duration of each activity. The findings were similar to [14], where the average stride duration was 5.6 s and each step duration was 1.2 s, hence the average velocity was 1.5 m/s. The recording equipment was sampling at 1500 Hz. Therefore, to achieve sufficient data sets, a minimum of 196 s per activity was deemed sufficient. This was an average of four minutes of walking and provided an average of 653 windows. Each window length was 350 ms. Therefore, each activity lasted about five minutes and every activity was repeated ten times. That is an average of twenty minutes of participation.

Statistical Analysis and Data Processing

The reduction of raw motion data was carried out using Noraxon MR3® software. A 2nd order Butterworth filter was used for the removal of specious markers and filtering the data using a cut-off frequency of 15 Hz. Temporal-spatial data such as speed, stance percentage, and step length was determined. Signal parameters such as mean, peak and minimum values were also determined. Kinetic data such as vertical ground reaction force and ankle, knee, and hip powers was compared with normative data [15].

Furthermore, Matlab functions were developed for post processing of the data and statistical analysis. The acquired data was analysed for skewness using the Pearson's coefficient of skewness;

$$\text{Pearson's coefficient of skewness, } a = \frac{(x_{mean} - x_{mode})}{x_{SD}}$$

Where xSD is the standard deviation, xmean and xmode are the mean values and mode of the variables. The data was considered normally distributed for $-0.5 < a < 0.5$. A paired t-test of unequal variance (level of significance, $p < 0.05$) was performed to determine whether there are significant differences between a normal subject and an amputee with a passive limb. The data was then evaluated to provide normative information for the amputee population when performing ambulatory related activities.

Results

The use of state of the art recording equipment such as the Noraxon Myomotion System and processing the data in MR3® minimised the need for excessive filtering. The sEMG signals recorded in MR3 system were exported to Matlab as csv files for further pre-processing. The results presented in this section include the characterisation of the sEMG signal, inertial measurements and the classifier performance. The development, training and testing of the pattern recognition control architecture followed the steps indicated in Figure 1.

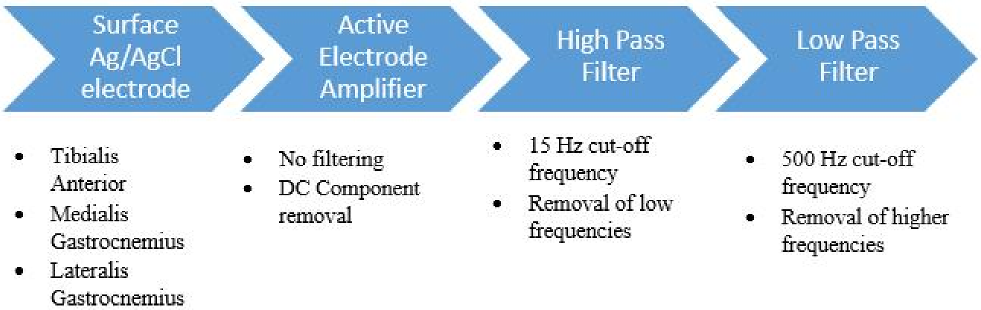

Figure 1: Signal acquisition flow, amplification and filtering from selected muscle sites

The filtering of the signal was achieved using Noraxon system at high pass filtering at 15Hz to eliminate noise as a result of skin movement. The removal of high frequencies was achieved using a low pass filter at 500Hz cut-off frequency. Filtering enhanced signal processing speed and quality as low and high frequencies due to noise interferences were eliminated.

The sEMG Signal Analysis On Oesteomyoplastic Transtibial Amputees

After amputation it was noted that not all residual muscles have the potential to have sEMG with sufficient power to be used as control signals. The sEMG signals recorded from the available three channels are illustrated in Figure 2.

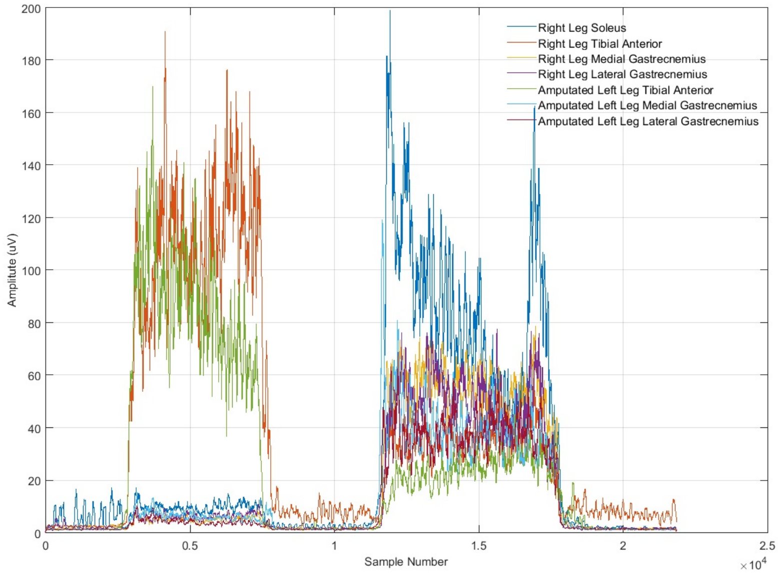

Figure 2: Comparison of mean amplitudes of rectified sEMG signals for the amputated and non-amputated leg

The active electrode had 15 Hz high pass filters. However, the signal presentation in Figure 2 was achieved after post-processing in Matlab using a 2nd order Butterworth filter. The active muscles on the amputated leg excludes the Soleus muscle which is dominant during plantarflexion on the non-amputated leg. In the absence of Soleus, the study utilised the Medialis and Lateralis Gastrocnemius and the comparison of the signal power of the Medialis Gastrocnemius muscle and the Soleus Muscle from the non-amputated leg is illustrated in Figure 3 below.

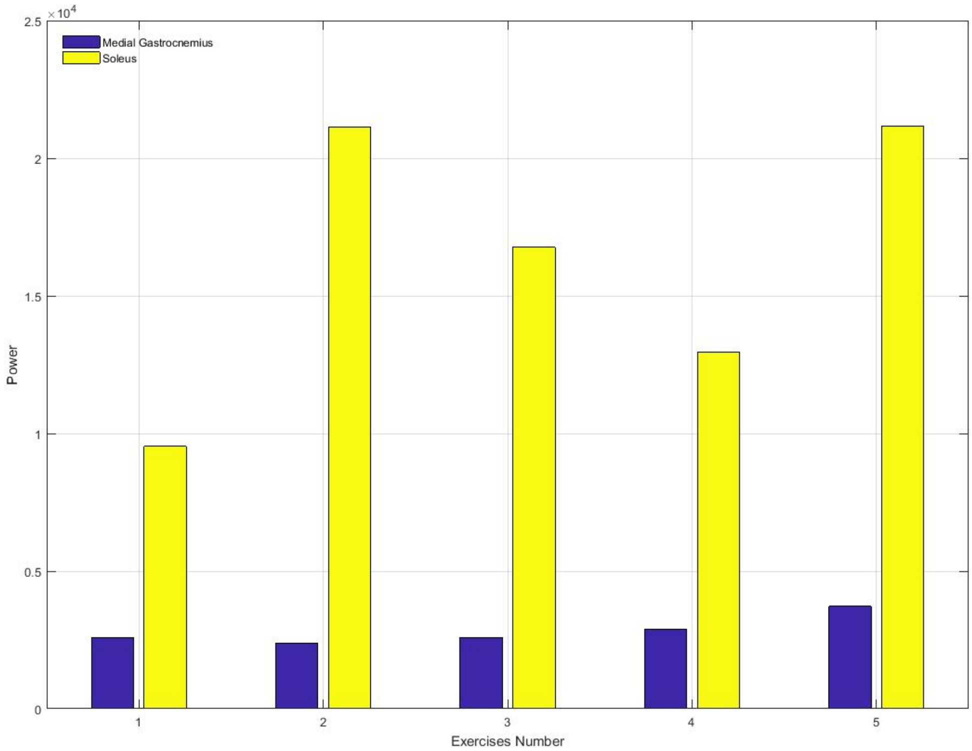

Figure 3: Comparison of signal power [W/Hz] between Soleus and Medialis Gastrocnemius muscles

The extraction of sEMG signals from an amputated leg is a challenge. The skin movement and changes in skin impedance contributed immensely to signal acquisition challenges. The effects of noise in the signal is illustrated in Figure 4.

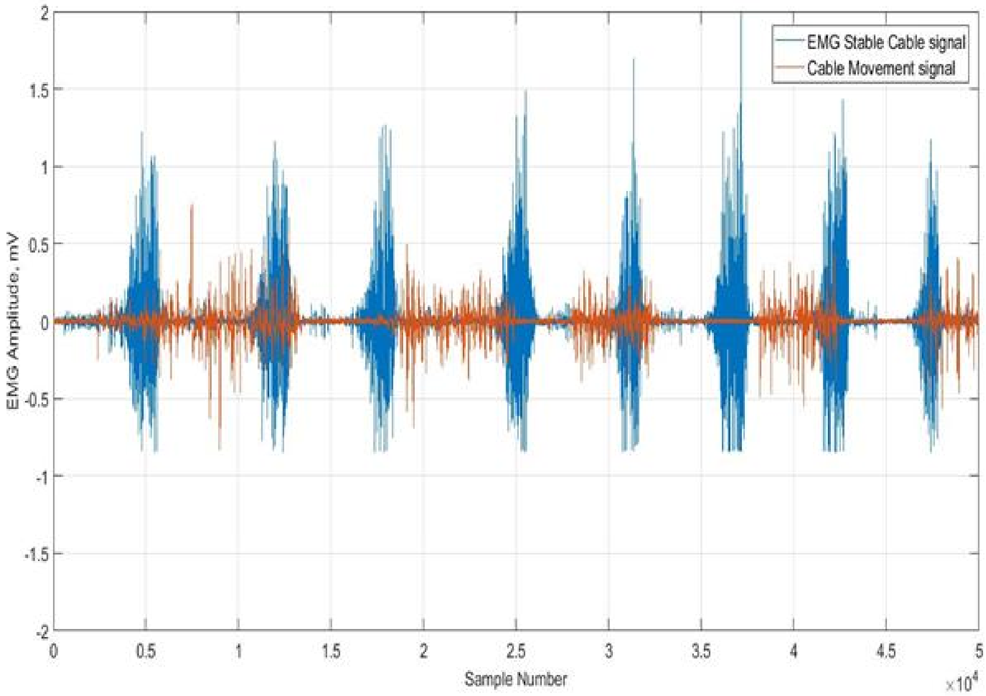

Figure 4: Comparison of a cable movement artefact and a clean signal during normal gait

The noise signal has direct effect on the quality of the extracted features and reduce the classification accuracy of the pattern recognition system. In order to achieve a clean signal, the surface area was cleaned using alcohol and the electrodes were firmly fixed on to the skin. However, issues regarding skin impedance could not be further improved. The quality of the sEMG signals used from the three channels is illustrated in Figure 5.

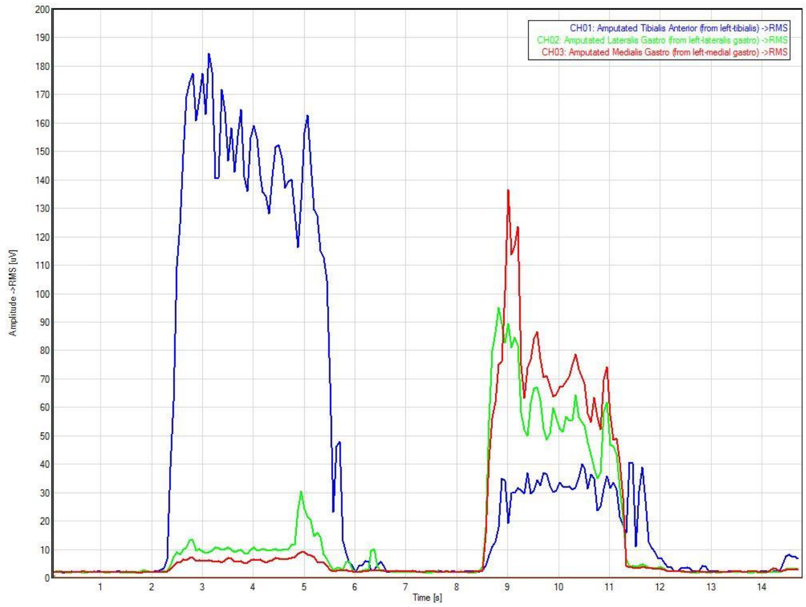

Figure 5: Filtered and rectified sEMG input signals to the feature extractor

The processed signal features were then used to extract relevant signal features that could improve distinction between dorsiflexion and plantarflexion movements.

Feature Extraction

The signals received by the controller from the analog front end were in vector format. As a result, data segmentation was initially implemented in order to improve the reliability of a feature vector. Furthermore, windowing positively affected the overall complexity and processing time of the architecture. When the data was recorded, it was in the form of a stream of digitalised values in a channel format. However, for analysis to be carried out there was a need to develop a window which focused on the motion of interest. As a result, a segment was regarded as a window where the features were extracted. The summation of all windows resulted in the length of the original signal. The analysis was applied to every window which was presented as a row within the feature vector and the result was a column of features for every window.

Features extracted include among them mean, standard deviation, root mean square value, mean absolute value, mean absolute deviation, zero crossing and slope sign change. The 250 ms window size with a 30 ms overlapping window was implemented and the processing time was less than 300 ms per window, as recommended by ISEK and SENIAM standards. The recorded signal length was restricted to over 17820 samples per exercise and this was done so as to achieve large data sets within small number of exercises so as to minimise the set-up times. The segmented data was then structured into a table format representing a matrix of *m* by *n* rows and columns. The rows *m* represented the signal window or segmented data. Then the selected features were applied for every window (row of values). The total number of samples in a window, N_{sw}, were determined as:

$$N_{sw} = t_w \times F_s$$

where t_w is the window length processing time and, for this study t_w = 250 ms and F_s was the sampling frequency which was 1500 Hz. Using these values, the derived number of samples in a standard window was 375 samples, as shown in Figure 6.

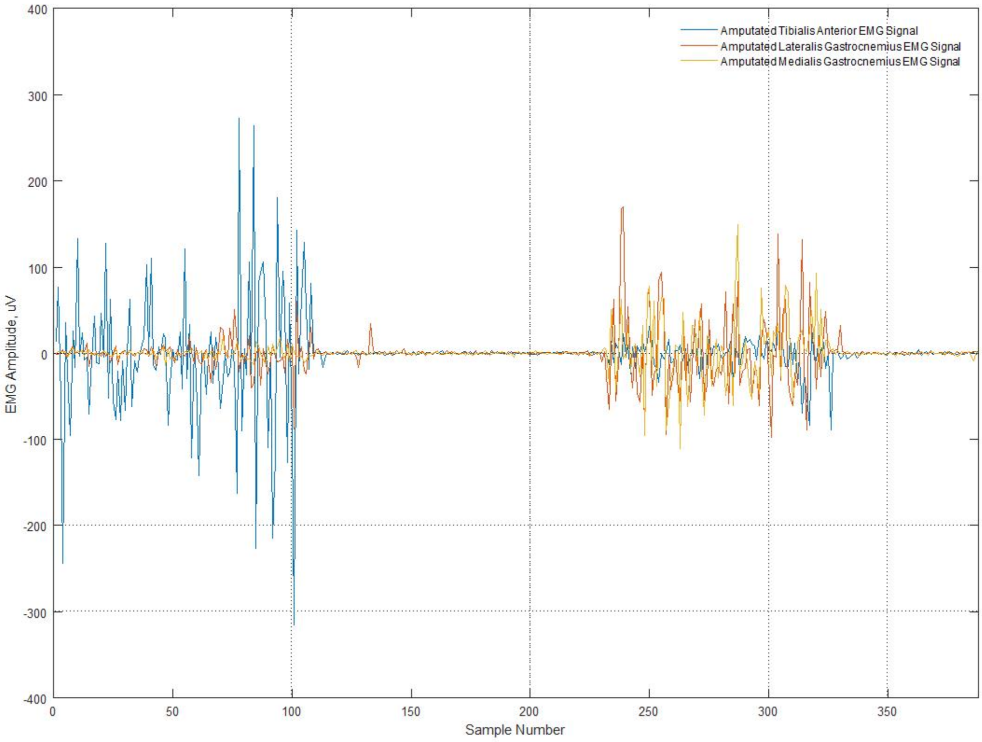

Figure 6: Window segmentation during ankle movement

The extracted feature values were combined into a single data set, x_{feat}, which was then used as an input data set to the classifier. A total of 11 extracted features were used to develop the feature vector. As a result, the total features for the whole control architecture were a product of a number of channels, *N*, and features per channel, x_{nf}, such that the feature vector had a total number of variables given by:

These features, x_F, were then used as an input vector to a classifier. The reliability of features to clearly provide distinction was evaluated using scatter plots as illustrated in Figure 7.

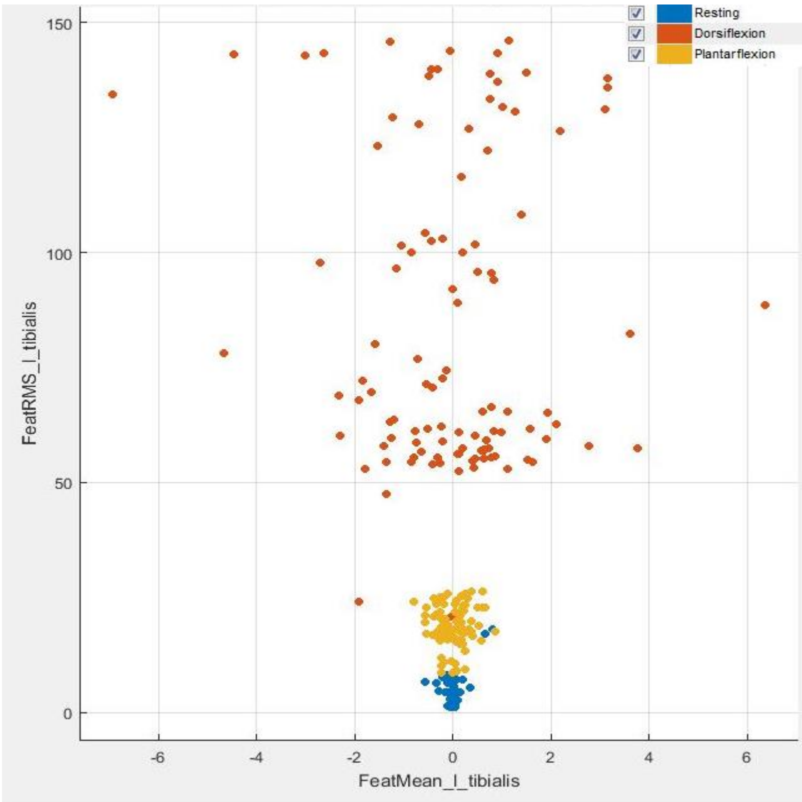

Figure 7: Feature analysis for sEMG signals from the Tibialis Anterior muscle

The behaviour of features however differed from one muscle to the other as illustrated in Figure 8 during the analysis of sEMG signals from Lateralis Gastrocnemius muscle.

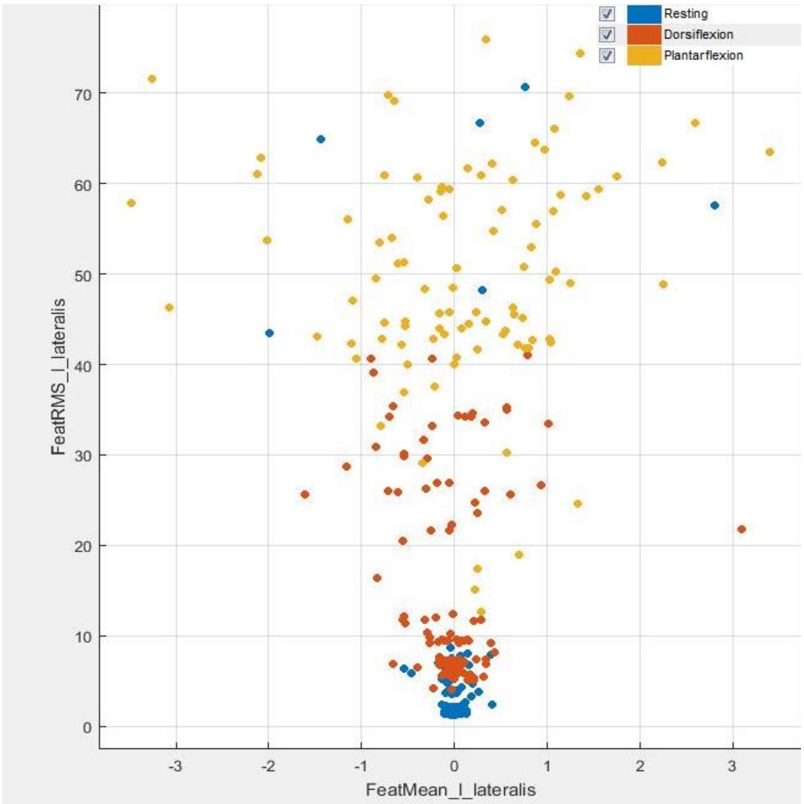

Figure 8: Feature analysis for sEMG signals from the Lateralis Gastrocnemius muscle

Figure 9 illustrates the use of *rms* and *std* of the signals to differentiate between dorsiflexion and plantarflexion movements. However, these two features were not sufficient to provide convincing classifier performance therefore eleven more features were tested.

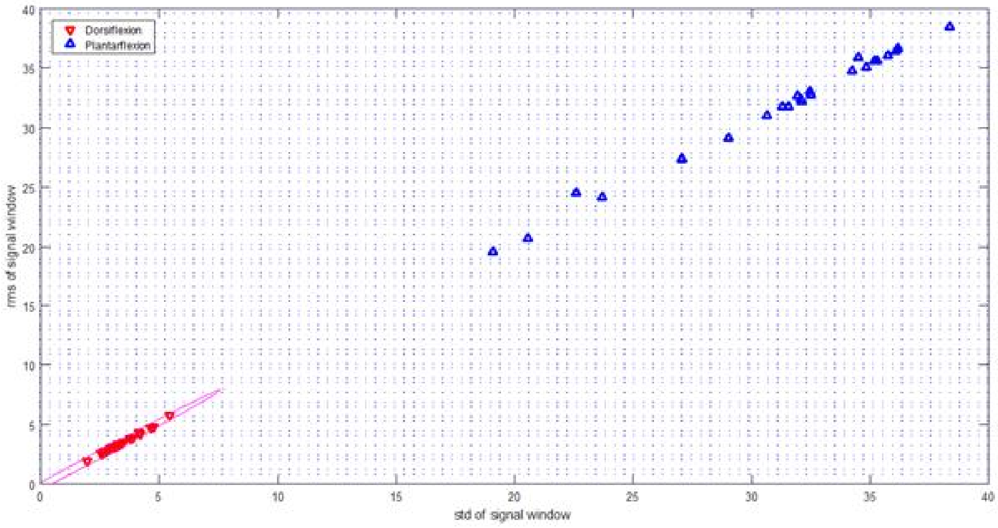

Figure 9: Using std and rms features to differentiate dorsiflexion and plantarflexion

It was deduced from the standard deviation (std) and root-mean-square (rms) values, extracted from labelled data for dorsiflexion and plantarflexion, that a hyperplane could be implemented. The linearity of the data was sufficient enough, to suggest Linear Support Vector Machine (LSVM) as the possible classifier. Therefore, all that was needed was to develop the optimal hyperplane that could maximise classifier performance even in the event of poorly presented features.

Classifier Performance

The performance of a classifier is determined by quality of the signal. However, the quality and choice of feature vectors also have an influence on the classifier performance in terms of response time, classification accuracy, specificity and sensitivity. The underlying principle for LSVM was to maximise the margin around the separating hyperplane by increasing the separating distance, d as illustrated in Figure 10. These support vectors (SV) had the capability of shifting the hyperplane, HP_0, when manipulated as compared to the other data points which were far from the hyperplane and not within the distance, *d*. The main role of the LSVM algorithm was to optimally determine the position of the hyperplane and widening the distance, *d*. Therefore, the problem becomes an optimisation problem which was solved using an optimisation technique. The input to the LSVM was a vector of features (x_{mean}, x_{std} ,..., x_{ISS}) extracted after application of PCA dimensionality reduction technique. The resultant output from the machine was a set of weights, w_i. Therefore, the hyperplanes were represented as follows:

$$HP_1 : w.x_i + b = +1$$
$$HP_2 : w.x_i + b = -1$$

Where **w**, was the weight vector, $\boldsymbol{x}$ is the input vector (features) and *b* was the bias.

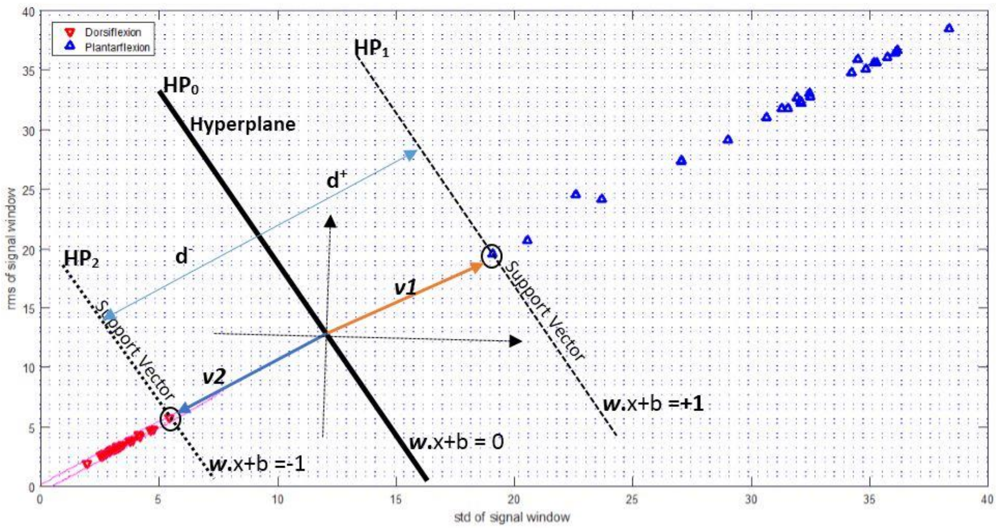

Figure 10: Illustration of LSVM technique on selected features.

Hence the HP_0 was regarded as the median, where w·xi+b=0. Therefore d^+ was the shortest distance to the closest positive point, while the shortest distance to the negative point was regarded as d- as a result $|d^+|+|d^-|=d$, which is the margin of separation that needs to be increased so as to optimise classifier performance. Assuming the generalised approach that the distance, d from a point (x0, y0) to any line Ax+By+c=0 on a Cartesian plane is be represented by;

$$d = \frac{Ax_0 + Bx_0 + c}{\sqrt{(A^2 + B^2)}}$$

And taking into consideration the hyper planes representing the support vectors, then the distance ,d^+ between HP_0 and HP_1 is derived as;

$$d^+ = \frac{|w.x + b|}{||w||} = \frac{1}{||w||}$$

As a result the total distance, d between HP1 and HP2 was given by;

$$d = \frac{2}{||w||}$$

Therefore when we maximised the margin, we simply maximised ‖w‖ given that there are no additional data points in between the two extreme hyper planes HP_1 and HP_2 such that;

$$HP_1 : \mathbf{w}.x_i + b \geq +1 when/ : y_i = +1$$
$$HP_2 : \mathbf{w}.x_i + b \leq -1 when/ : y_i = -1$$

Therefore the Linear SVM classifier for 2D discriminant was built on the basic form of;

$$f(x) = \mathbf{w}^{\mathrm{T}} x_i + b$$

For LSVM only the weight, w was returned after training for the classification of new EMG data which was presented as a vector of 23 features, $x_1, \ldots, x_n$. Therefore for linearly separable features;

$$f(x) = \sum_i \alpha_i y_i \left(x_i^T x \right) + b$$

Where α_i is a slack variable, $\mathbf{x}_i$ is the support vector and the data point is represented as ($\mathbf{x}_i$,y_i). During classification, 20% of the data set was used as validation data and 80% as training data. Each data set had approximately 388 observations, thus an average of 124,160 windows were used in the study during the development of the control architecture. There were several classifiers mentioned in the literature with regard to myoelectric signals classification. As a way of determining an optimum classifier, several classifiers were tested. Although the LSVM was the targeted classifier, Matlab Classification Learner was used to evaluate the performance of other classifiers on labelled data and the results are presented in Figure 11.

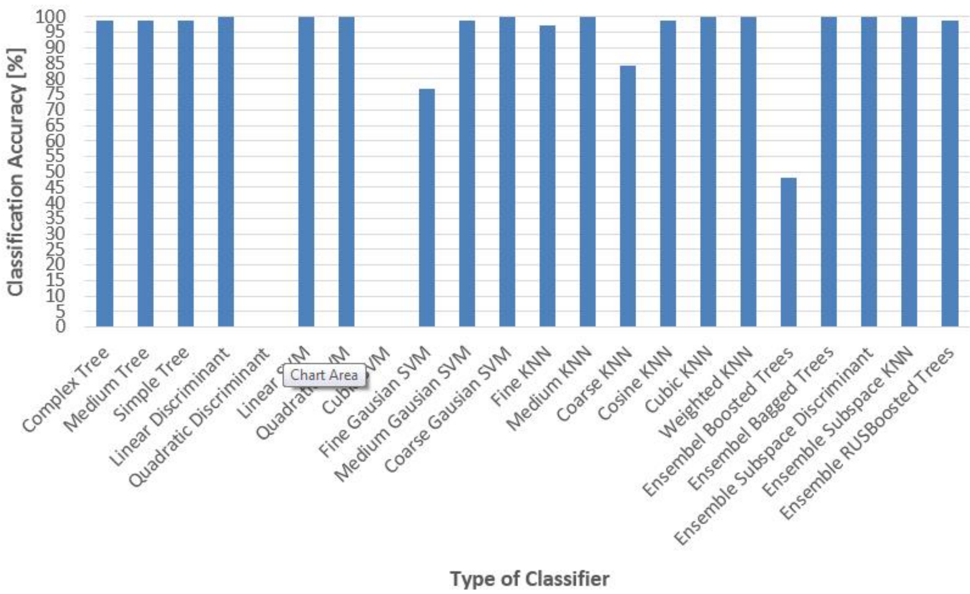

Figure 11: Average classifier perfomance based on all 11 features per channel in a 33 fature vector

Although all classifiers performed fairly good, the average processing time was then determined in an effort to further compare the classifiers. Figure 12 illustrates the average classifier processing times.

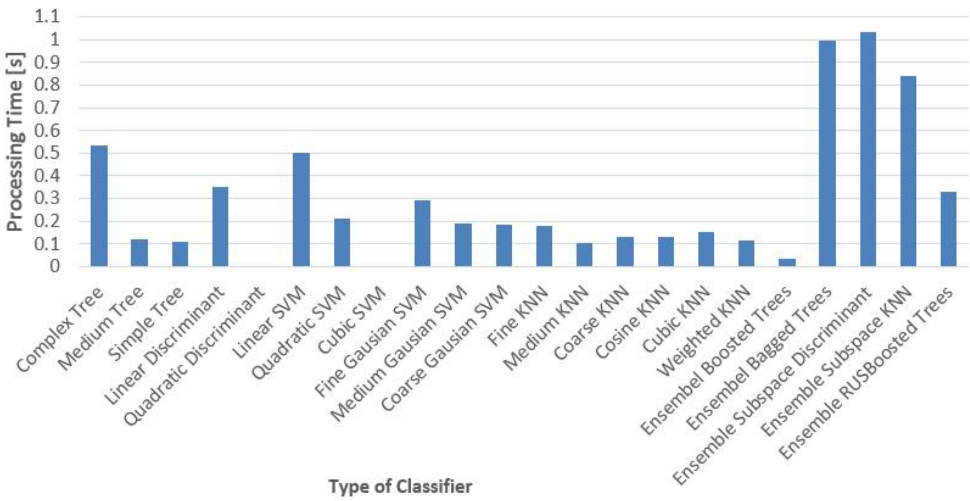

Figure 12: Average classifier processing times based on all 11 features per channel in a 33 fature vector

The Discriminant classifier had challenges with the nature of the features as a result it recorded 0 % classification accuracy. After the determination of classification accuracies and processing times, dimensionality reduction was implemented using Principle Component Analysis (PCA) in an effort to further reduce the processing times and improving classifier performance. The resulting classifier accuracy is illustrated in Figure 13.

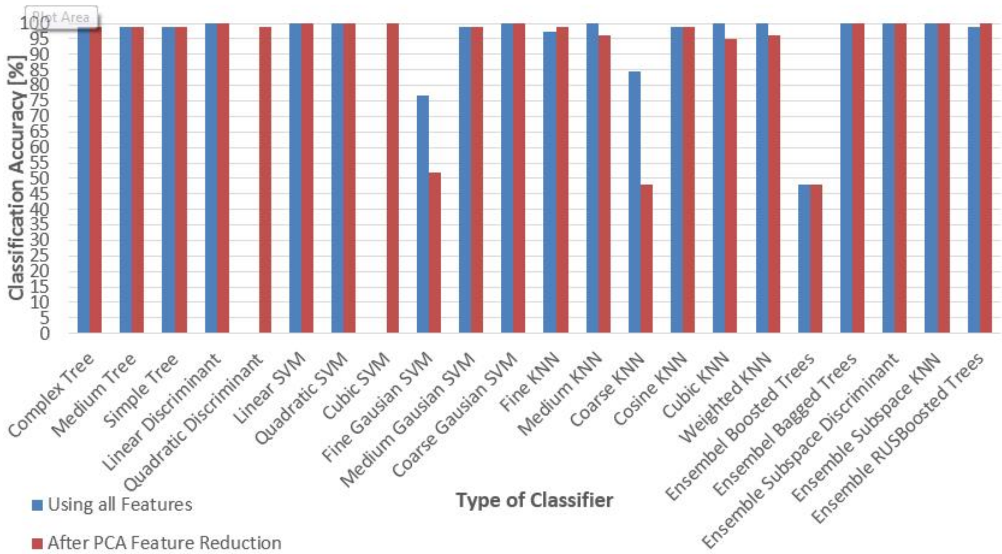

Figure 13: Classifier performance after the application of dimensionality reduction technique

Although there were notable changes in classifier accuracy, the processing times were also of major concern. Therefore, the resulting classifier performances are illustrated in Figure 14.

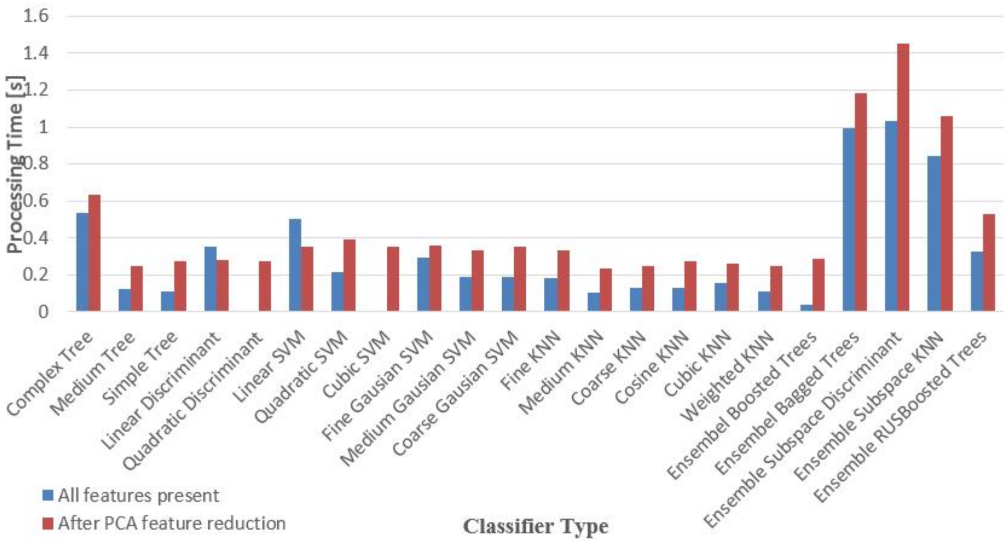

Figure 14: Classifier processing times after implementing PCA dimensionality reduction technique.

The Linear Discriminant classifier was able to classify the data after the removal of some features based on auto-regression coefficients. Although the performance of the classifier was reported in terms of classification accuracy and response time, other characteristics that were evaluated include sensitivity and specificity. These were clearly defined by the True Negative (TN), False Negative, (FN), True Positive (TP) and False Positive (FP). FN was regarded as invalid and TN as accurate.

$$TruePositive[TP] = ConditionPresent + PositiveResult$$

$$FalsePositive[FP] = ConditionAbsent + PositiveResult[TypeIerror]$$

$$FalseNegative[FN](invalid) = ConditionPresent{+}negativeResult[TypeIIerror]$$

$$TrueNegative[TN](accurate) = ConditionAbsent + NegativeResult$$

Therefore:

$$Precision\,(Class) = \frac{TP}{TP + FP}$$

$$Sensitivity\,(Class) = Recal\,(Class) = \frac{TP}{TP + FN}$$

$$Specificity\,(Class) = TrueNegativeRates\,(Class) = \frac{TN}{TN + FP}$$

The final averaged LSVM classification performance on test data is illustrated in Table 1 and Table 2. The classes of motion were namely (1) Dorsiflexion, (2) Plantarflexion and (3) Resting. Table 3 shows the confusion matrix of the classifier performance with a model accuracy of 99.25%. Figure 15 presents the classifier performance on labelled data.

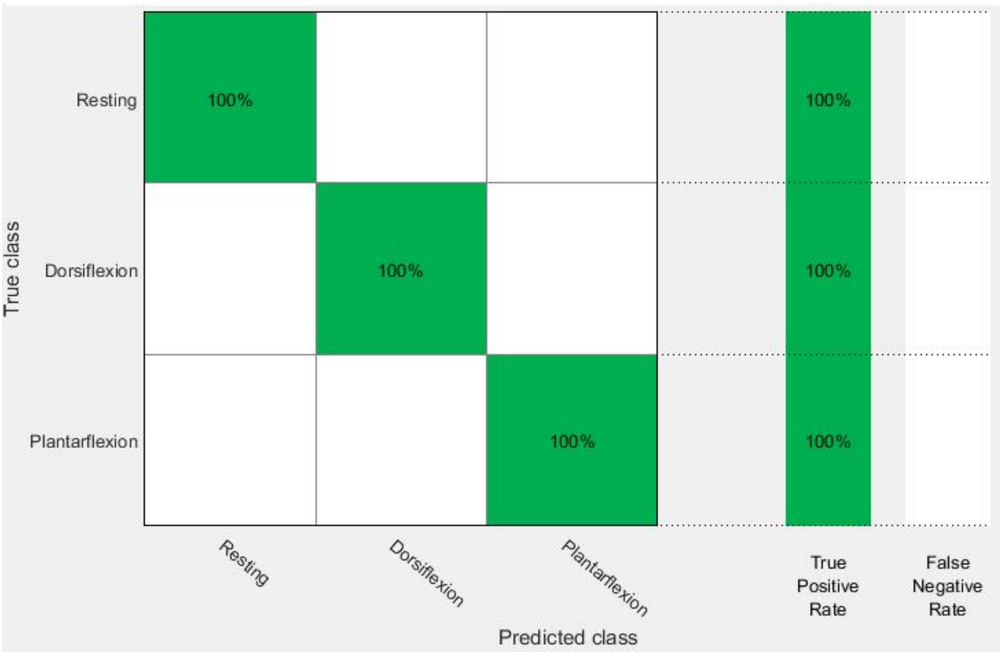

Figure 15: LSVM confusion matrix based on known labelled data.

Table 1: Classifier characteristics

Class	1	2	3
True Positive [TP]	262	101	119
False Positive [FP]	1	0	2
False Negative [FN]	1	1	1
True Negative [TN]	221	382	363

Table 2: Precision, sensitivity and specificity of the LSVM classifier on unknown data

Class	1	2	3
Precision	0.997881	1	0.97987
Sensitivity	0.996148	0.989035	0.995495
Specificity	0.997409	1	0.993989

Table 3: Confusion matrix of average trials based on unlabelled data

Rest	53.99843	0	0.116822
Dorsiflexion	0.997881	20.84382	0
Plantarflexion	0.996148	0.256677	24.57184
	Rest	**Dorsiflexion**	**Plantarflexion**

Discussion

The performance of a control system architecture is highly governed by performance of several modules within the system [16]. Hence forthwith, the quality of the input signal to the control system is of fundamental importance. The signal infidelity is one of the major concerns in myoelectric control systems. Figure 1 summarises the initial signal manipulations implemented before feature extraction during signal acquisition. The active filters were only implemented to remove the DC component of the signal. Sources of noise in sEMG acquisition are skin movement, changes in skin impedance and 50 Hz line interference. A high pass filter with a cut-off frequency of 15 Hz was able to remove low frequencies which are usually caused by skin and cable movements as illustrated in Figure 4 where the movement artefact was compared to an EMG signal. A 500 Hz Low pass filter was then implemented to complete a reliable 15-500 Hz band pass filter. The filtering was achieved with the aid of a 2nd order Sallen-Key architecture. Furthermore, an ADS1298 based signal processing module was implemented and the rectified and amplified signal is illustrated in Figure 5. A notch filter was not implemented to remove the 50Hz line interference as it was recommended by the ISEK and SENIAM standards that it would affect the signal quality although recent studies [17] highly recommends. The initial results of using a notch filter resulted in poor classifier performance.

Amputation of the lower limb is regarded as the last alternative for rehabilitation. However, in the event of lower limb amputation, the residual muscle within the stump will no longer possess the same signal strength [4] as the non-amputated leg as illustrated in Figure 2. The results shown in Figure 2, revealed that only Tibialis Anterior, Medialis Gastrocnemius and Lateralis Gastrocnemius muscle are the only muscles which could provide sEMG signals that could be used as input control signals to the control architecture. The amputation procedure made it difficult to access the Soleus muscle on the residual stump. However, Soleus muscles on the non-amputated leg possesses an average of 300% more energy and amplitude than the Medialis Gastrocnemius muscles as illustrated in Figure 3. The clear distinction between muscle performances is illustrated in Figure 5, and it is evident that Tibialis Anterior is dominant during dorsiflexion and Gastrocnemius muscles (Medialis and Lateralis) are dominant during plantarflexion movement. Such a distinction and stochastic nature of the sEMG signal proves that pattern recognition algorithms could be implemented.

One of the modules within a pattern recognition-based control system is the feature extractor. The success of the classifier highly depends on the quality of features extracted from the signal [18]. The features considered in this study were adapted from the features suggested by [19], which were an extension of the features used by [20]. Additionally, the modified Hudgins Features, suggested by [19], namely the Modified Mean Frequency (MMNF) and Modified Median Frequency (MMDF), were also considered so as to increase the feature vector with the aim of improving the classification accuracy. Windowing was applied with each window comprising of 375 samples as illustrated in Figure 6. The windowing technique [21] enabled easy extraction of the eleven features per channel resulting in thirty-three features. The larger the feature vector, the better the classification accuracy as illustrated in Figure 11. However, large feature vectors increase the processing times for certain features as shown in Figure 12. Dimensionality reduction technique implemented using PCA resulted in 30% reduction in processing time for LSVM as illustrated in Figure 14. This technique had no effect in terms of classification accuracy as shown on the performance of LSVM on Figure 11 and Figure 13 where the classification accuracy remained 100 % on average on labelled data.

Although classification accuracy is the main characteristic used in the literature to explain the classifier performance, sensitivity and specificity are other characteristics that assist on determining the classifier performance [22] as illustrated in Table 1 and Table 2. The sensitivity of the architecture illustrates how the system has the capability of changing the output signal based on the changes in the input signal. The specificity was above 99% for all movement classes, thus the architecture has the capability of assigning a decision from knowledge to a specific movement without assigning it to another movement class. The average classification accuracy of the LSVM system was 100% on known data as in Table 3. However, the LSVM achieved a fair 99.25% on unknown data.

In comparison with other previous studies, [20] used an Artificial Neural Network and achieved 91.2% for non-amputees and 85.5% on amputees and [23] reported 91.5% with 1 269.4 ms processing time which is almost four-fold the expected processing time. Other results were reported by [24] of 94-99% which was an average of 96.4% using upper limbs sEMG values. However, the difference is that the lower limb has to deal with supporting the body during locomotion which increased the probability of skin movement artefact. Therefore, the 0.75% classification error could not be reduced through continuous training due to variability in skin impedance, movement artefact and power line interference. The achieved 99.25% classification accuracy is sufficient for the clinical viability of the device.

The available literature revealed a lot of conflicting facts with regards to which feature domain to use between time features and frequency domain features. Ever since the 1990s [20] up to the recent studies [25], the size of a feature set has been a subject of debate [19], [26-28]. However, there is a common trend among all studies that the feature set was large enough to improve classification and small enough to reduce computation complexity. This has resulted in hybrid systems as new and existing techniques were merged together to improve classifier accuracy. It is, however, the use of several signal features in a classifier that usually enables robustness in a system although it increases transient response [29].

Conclusion

The use of pattern recognition control architectures presents an opportunity to implement machine intelligence. However, the study revealed that there are several issues that govern the performance of machine intelligence in a control architecture. These factors include the quality of the input signal, signal acquisition, processing techniques employed and the processing power of the main controller. It is, however, the performance of the pattern recognition technique used that determines the overall reliability of the control architecture.

A pattern recognition system based on myoelectric signal was developed and validated. The LSVM was modelled to accurately classify three motion classes (dorsiflexion, plantarflexion and resting) within the sagittal plane. The architecture is also composed of the principle component analysis (PCA) as a feature reduction module used during the training of the model. The use of PCA reduced the computational time and increased classification accuracy. The model classification accuracy on labelled data was 100%. However, on testing with unknown data, the architecture achieved 99.25% accuracy. The 0.75% error was attributed to variable properties of noise artefacts from cable movement, skin impedance and hardware components. Only the power-line interference remained constant across all data samples.

Therefore, the aforementioned results revealed that a robust pattern recognition control system is capable of classifying gait movements during walking, even in the event of noise interference.

References

1. Parmar N (2012) “Mind controlled bionic limbs bring giant strides in prosthetics,” The National, www.thenational.ae

2. Shi L, Liu X, Li N, Liu B, Liu Y (2013) Aging decreases the contribution of MaxiK channel in regulating vascular tone in mesenteric artery by unparallel downregulation of α-and β1-subunit expression. Mechanisms of ageing and development. 13: 416-25.

3. Blough DK, Hubbard S, McFarland LV, Smith DG, Gambel JM et al. (2010) Prosthetic cost projections for servicemembers with major limb loss from Vietnam and OIF/OEF. ARMY MEDICAL DEPT WASHINGTON DC; 2010 Jan.

4. Garikayi T, Van den Heever D, Matope S (2018) Analysis of surface electromyography signal features on osteomyoplastic transtibial amputees for pattern recognition control architectures. Biomedical Signal Processing and Control. 40: 10-22.

5. Dudley-Javoroski S, Shields RK (2008) Muscle and bone plasticity after spinal cord injury: review of adaptations to disuse and to electrical muscle stimulation. Journal of rehabilitation research and development.45: 283.

6. Mai A, Commuri S, Dionne CP, Day J, Ertl WJ et al. (2012) Effect of prosthetic foot on residuum-socket interface pressure and gait characteristics in an otherwise healthy man with transtibial osteomyoplastic amputation. JPO: Journal of Prosthetics and Orthotics. 24: 211-20.

7. Ferris AE (2016) Biomechanical Assessment of Ertl and Burgess Transtibial Amputation Techniques.

8. Czerniecki JM, Turner AP, Williams RM, Thompson ML, Landry G, et al. (2017) The development and validation of the AM-PREDICT model for predicting mobility outcome after dysvascular lower extremity amputation. Journal of vascular surgery. 65: 162-71.

9. Taylor BC, Poka A (2011) Osteomyoplastic transtibial amputation: technique and tips. Journal of orthopaedic surgery and research. 6: 13.

10. DeCoster TA, Homedan S (2006) Amputation osteoplasty. The Iowa orthopaedic journal. 26: 54.

11. Garikayi T, Van Den Heever D, Matope S (2017) Investigating the effects of passive mechanical ankle on unilateral osteomyoplastic transtibial amputees. Journal of Musculoskeletal Research. 20: 1750015.

12. Merletti R, Di Torino P (1999) Standards for reporting EMG data. J Electromyogr Kinesiol. 9: 3-4.

13. Stegeman D, Hermens H (2007) Standards for surface electromyography: The European project Surface EMG for non-invasive assessment of muscles (SENIAM). Enschede: Roessingh Research and Development. 108-2.

14. Bateni H, Olney SJ (2002) Kinematic and kinetic variations of below-knee amputee gait. JPO: Journal of Prosthetics and Orthotics. 14: 2-10.

15. Kosse NM, Vuillerme N, Hortobágyi T, Lamoth CJ (2016) Multiple gait parameters derived from iPod accelerometry predict age-related gait changes. Gait & posture. 46: 112-7.

16. Gu Y, Yang D, Huang Q, Yang W, Liu H (2018) Robust EMG pattern recognition in the presence of confounding factors: features, classifiers and adaptive learning. Expert Systems with Applications. 96: 208-17.

17. Mewett DT, Nazeran H, Reynolds KJ (2001) Removing power line noise from recorded EMG. InEngineering in Medicine and Biology Society, 2001. Proceedings of the 23rd Annual International Conference of the IEEE 2001, 3: 2190-2193.

18. Phinyomark A, Limsakul C, Phukpattaranont P (2009) A novel feature extraction for robust EMG pattern recognition. arXiv preprint arXiv:0912.3973.

19. Chowdhury RH, Reaz MB, Ali MA, Bakar AA, Chellappan K et al. (2013) Surface electromyography signal processing and classification techniques. Sensors. 13: 12431-66.

20. Hudgins B, Parker P, Scott RN (1993) A new strategy for multifunction myoelectric control. IEEE Transactions on Biomedical Engineering. 40: 82-94.

21. Dalir A, Beheshti AA, Masoom MH (2018) Classification of vehicles based on audio signals using quadratic discriminant analysis and high energy feature vectors. arXiv preprint arXiv:1804.01212.

22. Polat K, Güneş S (2007) Classification of epileptiform EEG using a hybrid system based on decision tree classifier and fast Fourier transform. Applied Mathematics and Computation. 187: 1017-26.

23. Nishikawa D, Yu W, Yokoi H, Kakazu Y (1999) EMG prosthetic hand controller using real-time learning method. InSystems, Man, and Cybernetics, 1999. IEEE SMC'99 Conference Proceedings. 1999 IEEE International Conference on 1999 1: 153-8.

24. Ajiboye AB, Weir RF (2005) A heuristic fuzzy logic approach to EMG pattern recognition for multifunctional prosthesis control. IEEE Transactions on Neural Systems and Rehabilitation Engineering. 13: 280-91.

25. Rosli NA, Rahman MA, Balakrishnan M, Mazlan SA, Zamzuri H (2017) The fusion of HRV and EMG signals for automatic gender recognition during stepping exercise. Telkomnika. 15: 756.

26. Englehart K, Hudgins B (2003) A robust, real-time control scheme for multifunction myoelectric control. IEEE transactions on biomedical engineering. 50: 848-54.

27. Englehart K, Hugdins B, Parker P (2000) Multifunction control of prostheses using the myoelectric signal. Intelligent systems and technologies in rehabilitation engineering. 153-208.

28. Phinyomark A, Phukpattaranont P, Limsakul C (2012) Feature reduction and selection for EMG signal classification. Expert Systems with Applications. 39: 7420-31.

29. Phinyomark A, Scheme E (2018) A feature extraction issue for myoelectric control based on wearable EMG sensors. InSensors Applications Symposium (SAS), 1-6.